An Unconditionally Stable Extended (USE) Finite-Element Time-Domain Solution of Active Nonlinear Microwave Circuits Using Perfectly Matched Layers

Hsiao-Ping Tsai, *Student Member, IEEE,* Yuanxun Wang, *Member, IEEE*, and Tatsuo Itoh, *Fellow, IEEE*

***Abstract*—This paper proposes an extension of the unconditionally stable finite-element time-domain (FETD) method for the global electromagnetic analysis of active microwave circuits. This formulation has two advantages. First, the time-step size is no longer governed by the spatial discretization of the mesh, but rather by the Nyquist sampling criterion. Second, the implementation of the truncation by the perfectly matched layers (PML) is straightforward. An anisotropic PML absorbing material is presented for the truncation of FETD lattices. Reflection less than −50 dB is obtained numerically over the entire propagation bandwidth in waveguide and microstrip line. A benchmark test on a microwave amplifier indicates that this extended FETD algorithm is not only superior to finite-difference time-domain-based algorithm in mesh flexibility and simulation accuracy, but also reduces computation time dramatically.**

***Index Terms*—Active/nonlinear circuit simulation, finite-element time-domain method, global modeling, PML.**

I. Introduction

RECENT trend in the microwave and very large scale integration (VLSI) industries is to design faster circuits and to integrate many functions in a single design. Consequently, designs are made with higher operating frequencies, faster digital clock rate, smaller device sizes, and lower power consumption. These aspects make the signal integrity analysis a challenging task and highlight the interconnect effects, such as ringing, signal delay, distortion, reflections, and crosstalk. These effects must be included in the early design stage. At very high frequencies, lumped and distributed interconnect models based on quasi-TEM approximations will become inaccurate and cannot be rigorously analyzed with currently available software. Accurate analysis of complex circuit structures such as a monolithic microwave integrated circuit requires a sophisticated mixed full-wave electromagnetic (EM) and circuit simulator able to account for the EM coupling between the closely placed components and all boundary conditions.

Extensive investigations have been proposed in the literature aiming at the mixed EM and circuit analysis algorithms. It is often important to analyze systems in a broad frequency band. Time-domain methods are well suited to achieve this target because they can obtain broad-band information from a single computation. These transient approaches can be classified into the following three categories:

1) transmission-line matrix method [1], [2];
2) finite-difference time-domain (FDTD)-based algorithms;
3) finite-element method (FEM)-based algorithms.

The vast majority of researchers focused on the extension of the FDTD techniques to include lumped elements [3], [4]. The combination of FDTD and SPICE is proposed in [5]. The problem of using SPICE is that programming the link between the EM simulator and SPICE can be time consuming. Several extended FDTD algorithms are proposed in [6]–[8] without SPICE. An algorithm based on the equivalent-source concept for incorporating active devices into the FDTD method is presented in [7]. This algorithm has been applied to solve nonlinear microwave circuits including amplifiers and mixers [9], [10], accounting also for crosstalk and packaging effects [10]. The principal advantage of the FDTD is ease of implementation. However, in its conventional form, the grid for the spatial discretization is Cartesian and uniform in nature. Consequently, FDTD restricts geometry representation to stair-stepped-shaped boundaries, which results in a large burden on the memory resources and the CPU time when the method is applied to geometries with curvature and/or fine features.

In the second category, the harmonic-balance method for extending the finite-element scheme in the frequency domain to include passive linear components has been presented by Guillouard *et al.* in [11]. The same author also developed an algorithm combining the FEM with SPICE in the time domain [12]. Chang *et al.* [13] proposed an extension of the finite-element time-domain (FETD) method for solving nonlinear microwave circuits without using SPICE. The FETD method combines the advantages of a time-domain technique and the versatility of their spatial discretization procedures. The comparison between FDTD, FETD, and measurement results has been shown in [13] that the FETD scheme provides better accuracy than FDTD-based techniques reported thus far. However, the time step required to converge to a final solution is smaller than those required by explicit FDTD methods due to conditional stability [14]. Gedney and Navsariwala [15] proposed an implicit FETD solution based on the second-order electric-field Maxwell's equation. The time-dependent formulation employs a time-integration method based on the Newmark–Beta method.

Manuscript received September 6, 2001; revised November 23, 2001.

The authors are with the Department of Electrical Engineering, University of California at Los Angeles, Los Angeles, CA 90095 USA.

Digital Object Identifier 10.1109/TMTT.2002.803442.

With appropriate values of the parameters controlling the accuracy and stability of the scheme, the Newmark method yields an unconditionally stable scheme with second-order accuracy.

In this paper, we propose an unconditionally stable extended finite-element time-domain (USE FETD) method to solve microwave passive/active circuits by adapting the lumped-element treatment proposed by Chang *et al.* [13]. A benchmark test on a microwave amplifier has been compared with results in [13] and shows that this scheme not only retains the high accuracy of the FETD, but also significantly reduces computation time over the conditionally stable FETD method by at least ten times.

One of the most important aspects of finite-difference and finite-element implementations is the truncation of the computational volume. An ideal truncation scheme must ensure that the outgoing waves are not reflected backward at the mesh termination surface. To date, a variety of absorbing boundary conditions (ABCs) have been employed for truncating the computational volume. There are several difficulties with traditional ABCs. For example, to terminate the microwave circuit requires *a priori* knowledge of the propagation constants that are typically not available for high-density packages. Also, when used to terminate an open domain, ABCs reduce the convergence rate and may be hard to implement on a surface conformal to the scatter or radiator.

An alterative to traditional ABCs is to employ an artificial absorber for mesh truncation. Berenger [16] introduced an approach of an artificial absorber, called perfectly matched layers (PML), which is reflectionless at its surface for all incident angles. However, Berenger's PML does not satisfy Maxwell's equations and cannot be easily implemented in a finite-element solution. Sacks *et al.* [17] presented an alternative approach for deriving a PML for mesh truncation. This approach is based on using anisotropic material properties (μ, ε, σE, σM) to describe the absorbing layer. In contrast to the former PML approach, this approach does not require a modification of Maxwell's equations. Furthermore, implementation of the anisotropic PML approach is straightforward. Sacks' method is widely used in the FEM in the frequency domain [18], and was extended to the FDTD method by Gedney [19].

PMLs for FETD have not received much attention, except by Mathis [20]. Thus far, there is no detailed study in terms of the quality of a PML in the FETD scheme. In this paper, we adapt Mathis's anisotropic PML to truncate the simulation volume in the global EM analysis of active microwave circuits. Numerical results of propagation in a waveguide and a microstrip structure are given to demonstrate the performance of an optimized PML.

This paper is organized as follows. Section II presents the FETD formulation implementing an anisotropic PML absorption material, as well as the algorithm coupling with lumped passive/active linear/nonlinear components. Section III illustrates some numerical examples to demonstrate the PML performance, followed by the full-wave simulation results of a microwave amplifier. Finally, conclusions are drawn in Section IV.

II. Theory

A. Anisotropic PML for FETD Formulation

This section derives the FETD formulation to be used when the perfectly matched anisotropic absorber is employed to terminate the computational domain. The general time–harmonic form of Maxwell's equations is

$$\begin{aligned}\nabla\times\mathbf{E}&=-j\omega[\mu]\mathbf{H}-[\sigma_M]\mathbf{H}=-j\omega[\overline{\mu}]\mathbf{H}\\ \nabla\times\mathbf{H}&=j\omega[\varepsilon]\mathbf{E}+[\sigma_E]\mathbf{E}+\mathbf{J}_i=j\omega[\overline{\varepsilon}]\mathbf{E}+\mathbf{J}_i\end{aligned}\tag{1}$$

where $[\overline{\mu}]$ and $[\overline{\varepsilon}]$ are complex diagonal tensors of permeability and permittivity, respectively. In this section, we concentrate on the materials with $[\overline{\mu}]$ and $[\overline{\varepsilon}]$ diagonal in the same coordinate system. To match the intrinsic impedance of the anisotropic PML medium to free space, the condition

$$\frac{[\overline{\varepsilon}]}{\varepsilon_0}=\frac{[\overline{\mu}]}{\mu_0}\tag{2}$$

must hold. Consequently, the tensors $[\overline{\mu}]$ and $[\overline{\varepsilon}]$ can be written as

$$[\overline{\varepsilon}]=\varepsilon[\Lambda]\quad[\overline{\mu}]=\mu[\Lambda]\tag{3}$$

where

$$[\Lambda]=\begin{bmatrix}\dfrac{S_yS_z}{S_x}&0&0\\0&\dfrac{S_xS_z}{S_y}&0\\0&0&\dfrac{S_yS_x}{S_z}\end{bmatrix}\quad S_{x,y,z}=1+\frac{\sigma_{x,y,z}}{j\omega\varepsilon_0}.$$

Since we want to consider only the electric field in the calculation domain, Maxwell's equations can be written as

$$\nabla\times\frac{1}{\mu}\left([\Lambda]^{-1}\cdot\nabla\times\mathbf{E}\right)-\omega^2\varepsilon[\Lambda]\mathbf{E}=-j\omega\mathbf{J_i}.\tag{4}$$

Using (4) as the starting point, we can obtain a modified equation, which can be utilized to derive the time-domain formulation. Next, we want to isolate the dependencies in order to go to a temporal formulation

$$\begin{aligned}\nabla\times\frac{1}{\mu}\nabla\times\mathbf{E}+\frac{2}{j\omega\varepsilon_0}\nabla\times\frac{1}{\mu}[I]\nabla\times\mathbf{E}-\frac{1}{\omega^2\varepsilon_0^2}\nabla\times\frac{1}{\mu}[I]^2\nabla\times\mathbf{E}\\ =\omega^2\varepsilon\mathbf{E}+\frac{2\omega\varepsilon}{j\varepsilon_0}[J]\mathbf{E}-\frac{\varepsilon}{\varepsilon_0^2}([J]+2[K])\mathbf{E}-\frac{2\varepsilon}{j\omega\varepsilon_0^2}[L]\mathbf{E}\\ +\frac{\varepsilon}{\omega^2\varepsilon_0^4}[K]^2\mathbf{E}-j\omega\mathbf{J_i}\end{aligned}\tag{5}$$

where

$$[I]=\begin{bmatrix}\sigma_x&0&0\\0&\sigma_y&0\\0&0&\sigma_z\end{bmatrix}$$

$$[J]=\begin{bmatrix}\sigma_y+\sigma_z&0&0\\0&\sigma_z+\sigma_x&0\\0&0&\sigma_x+\sigma_y\end{bmatrix}$$

$$[K]=\begin{bmatrix}\sigma_y\sigma_z&0&0\\0&\sigma_z\sigma_x&0\\0&0&\sigma_x\sigma_y\end{bmatrix}$$

$$[L]=\begin{bmatrix}(\sigma_y+\sigma_z)\sigma_y\sigma_z&0&0\\0&(\sigma_z+\sigma_x)\sigma_z\sigma_x&0\\0&0&(\sigma_x+\sigma_y)\sigma_x\sigma_y\end{bmatrix}.$$

To solve (5) numerically, we discretize the domain with tetrahedral elements and express the electric field in terms of basis functions associated with the edges of the elements

$$\mathbf{E} = \sum_{i=1}^{N} W_i^{(1)} e_i \tag{6}$$

where N is the total number of the edges, $W_i^{(1)}$, i.e., a one-form Whitney edge element [21], [22], is the vector basis function associated with edge i, and e_i is the circulation of the electric field along the edge i.

The next step is to convert the frequency-domain formulation to the time-domain version using the following relations:

$$j\omega \leftrightarrow \frac{\partial}{\partial t} \quad -\omega^2 \leftrightarrow \frac{\partial^2}{\partial t^2} \quad \frac{1}{j\omega} \leftrightarrow \int_t \quad \frac{-1}{\omega^2} \leftrightarrow \iint_t . \tag{7}$$

Applying the above transformation, we can recast the Maxwell's equation in the following form:

$$\begin{aligned}\nabla \times \frac{1}{\mu} \nabla \times \mathbf{E} + \frac{2}{\varepsilon_0} \nabla \times \frac{1}{\mu} [I] \nabla \times \int_t \mathbf{E} + \frac{1}{\varepsilon_0^2} \nabla \times \frac{1}{\mu} [I]^2 \nabla \\ \times \iint_t \mathbf{E} + \varepsilon \frac{\partial^2 \mathbf{E}}{\partial t^2} + \frac{2\varepsilon}{\varepsilon_0} [J] \frac{\partial \mathbf{E}}{\partial t} + \frac{\varepsilon}{\varepsilon_0^2} \left([J]^2 + 2[K]\right) \mathbf{E} \\ + \frac{2\varepsilon}{\varepsilon_0^3} [L] \int_t \mathbf{E} + \frac{\varepsilon}{\varepsilon_0^4} [K]^2 \iint_t \mathbf{E} = -\frac{\partial \mathbf{J}_i}{\partial t}.\end{aligned} \tag{8}$$

Testing (8) with edge basis function $W^{(1)}$, associated with nonperfect-electric-conductor (PEC) edges of the grid, integrating by parts, and decomposing the unknown field $\mathbf{E}$ in a finite-element basis yields the following weak form:

$$[A]\underline{e} + [B] \frac{d\underline{e}}{dt} + [C] \frac{d^2 \underline{e}}{dt^2} + [D]\underline{f} + [E]\underline{g} = -\frac{\partial \underline{I}}{\partial t} \tag{9}$$

where $\underline{e}$ is the vector of unknowns, $\underline{I}$ is the vector of excitation currents or the lumped-element current, and $[A]$, $[B]$, $[C]$, $[D]$, and $[E]$ are time-independent matrices. Those terms are given by

$$\begin{aligned}[A]_{ij} &= \int_V \frac{1}{\mu} \nabla \times W_i^{(1)} \cdot \nabla \times W_j^{(1)} + \frac{\varepsilon}{\varepsilon_0^2} \left([J]^2 + 2[K]\right) W_i^{(1)} \cdot W_j^{(1)} \, dV \\ [B]_{ij} &= \int_V \frac{2\varepsilon}{\varepsilon_0} [J] W_i^{(1)} \cdot W_j^{(1)} \, dV, \\ [C]_{ij} &= \int_V W_i^{(1)} \cdot W_j^{(1)} \, dV \\ [D]_{ij} &= \int_V \frac{2}{\mu \varepsilon_0} [I] \nabla \times W_i^{(1)} \cdot \nabla \times W_j^{(1)} + \frac{2\varepsilon}{\varepsilon_0^3} [L] W_i^{(1)} \cdot W_j^{(1)} \, dV \\ [E]_{ij} &= \int_v \frac{1}{\mu \varepsilon_0^2} [I]^2 \nabla \times W_i^{(1)} \cdot \nabla \times W_j^{(1)} + \frac{\varepsilon}{\varepsilon_0^4} [K]^2 W_i^{(1)} \cdot W_j^{(1)} \, dV \\ [I]_i &= \int_V W_i^{(1)} \cdot \frac{\partial \mathbf{J}_i}{\partial t} \, dV \\ \underline{f} &= \int_t \underline{e} \, dt \\ \underline{g} &= \iint_t \underline{e} \, dt.\end{aligned}$$

B. Mixed Full-Wave EM and Passive/Active Device Analysis

In order to introduce lumped elements into the three-dimensional (3-D) FETD simulator, all vectors and matrices have been split to separate the unknowns associated to edges in the mesh in which the lumped elements are located (denoted by the subscript c) from those associated to standard edges (subscript e). Based on the method of Chang *et al.* [13], (9) can be recast into the following form:

$$\begin{aligned}&\begin{bmatrix}[A]_{ee}[A]_{ec} \\ [A]_{ce}[A]_{cc}\end{bmatrix} \begin{bmatrix}\underline{e_e} \\ \underline{e_c}\end{bmatrix} + \begin{bmatrix}[B]_{ee}[B]_{ec} \\ [B]_{ce}[B]_{cc}\end{bmatrix} \cdot \frac{\partial}{\partial t} \begin{bmatrix}\underline{e_e} \\ \underline{e_c}\end{bmatrix} + \begin{bmatrix}[C]_{ee}[C]_{ec} \\ [C]_{ce}[C]_{cc}\end{bmatrix} \\ &\quad \cdot \frac{\partial^2}{\partial t^2} \begin{bmatrix}\underline{e_e} \\ \underline{e_c}\end{bmatrix} + \begin{bmatrix}[D]_{ee}[D]_{ec} \\ [D]_{ce}[D]_{cc}\end{bmatrix} \begin{bmatrix}\underline{f_e} \\ \underline{f_c}\end{bmatrix} + \begin{bmatrix}[E]_{ee}[E]_{ec} \\ [E]_{ce}[E]_{cc}\end{bmatrix} \begin{bmatrix}\underline{g_e} \\ \underline{g_c}\end{bmatrix} \\ &\quad = \begin{bmatrix}\partial \underline{I_e}/\partial t \\ \partial \underline{I_c}/\partial t\end{bmatrix}\end{aligned} \tag{10}$$

where $[B]_{ec}$, $[B]_{ce}$, $[B]_{cc}$, $[D]_{ec}$, $[D]_{ce}$, $[D]_{cc}$, $[E]_{ec}$, $[E]_{ce}$, $[E]_{cc}$, $\underline{f}_c$, and $\underline{g}_c$ are zero since the lump circuits are not inside the perfectly matched anisotropic absorber. $\underline{I}_e$ is zero if there is no excitation in the passive structure. $\underline{I}_c$ and $\underline{e}_c$ are the current and voltage at the terminal of the lumped element included in the computational domain, respectively. Based on the Newmark–Beta formulation [23], [24], (10) is approximated as

$$\begin{aligned}&[A]_{ee}\left[\beta \underline{e_e}^{n+1} + (1-2\beta)\underline{e_e}^{n} + \beta \underline{e_e}^{n-1}\right] + [A]_{ec}\underline{e_c} \\ &\quad + [B]_{ee} \frac{\underline{e_e}^{n+1} - \underline{e_e}^{n-1}}{2\Delta t} + [C]_{ee} \frac{\underline{e_e}^{n+1} - 2\underline{e_e}^{n} + \underline{e_e}^{n-1}}{\Delta t^2} \\ &\quad + [C]_{ec} \frac{\partial^2 \underline{e_c}}{\partial t^2} + [D]_{ee}\underline{f_e}^{n} + [E]_{ee}\underline{g_e}^{n} \\ &\quad = -\frac{\partial \underline{I_e}}{\partial t}\end{aligned} \tag{11}$$

$$\begin{aligned}&[A]_{ce}\left[\beta \underline{e_e}^{n+1} + (1-2\beta)\underline{e_e}^{n} + \beta \underline{e_e}^{n-1}\right] + [A]_{cc}\underline{e_c} \\ &\quad + [C]_{ce} \frac{\underline{e_e}^{n+1} - 2\underline{e_e}^{n} + \underline{e_e}^{n-1}}{\Delta t^2} + [C]_{cc} \frac{\partial^2 \underline{e_c}}{\partial t^2} \\ &\quad = -\frac{\partial \underline{I_c}}{\partial t}\end{aligned} \tag{12}$$

where

$$\begin{aligned}\underline{f_e^n} &= \underline{f_e}^{n-1} + \frac{\Delta t}{2} \underline{e_e}^{n-1} + \frac{\Delta t}{2} \underline{e_e}^{n} \\ \underline{g_e^n} &= \underline{g_e}^{n-1} + \Delta t \underline{e_e}^{n-1} + \frac{\Delta t^2}{4} \underline{e_e}^{n-1} + \frac{\Delta t^2}{4} \underline{e_e}^{n}.\end{aligned} \tag{13}$$

Gedney and Navsariwala [15] has proven that unconditional stability is achievable by choosing the interpolation parameter $\beta \geq 1/4$. This allows the time step to be chosen in order to give a specific accuracy without being constrained by stability criteria. It was further shown that choosing $\beta = 1/4$ minimized solution error. Substituting $\underline{e}_e^{n+1}$ in (11) into (12) yields a set of second-order ordinary differential equations (ODEs) in terms of unknown $\underline{e}_c$ as follows:

$$\left[\underline{C_d}\right] \frac{\partial^2 \underline{e_c}}{\partial t^2} + \frac{\partial \underline{I_c}}{\partial t} = [\underline{F}]. \tag{14}$$

To solve the above second-order ODE, let

$$\underline{I_d} = \left[\underline{C_d}\right] \frac{\partial \underline{e_c}}{\partial t} + \underline{I_c} \quad \frac{\partial \underline{I_d}}{\partial t} = [\underline{F}] \tag{15}$$

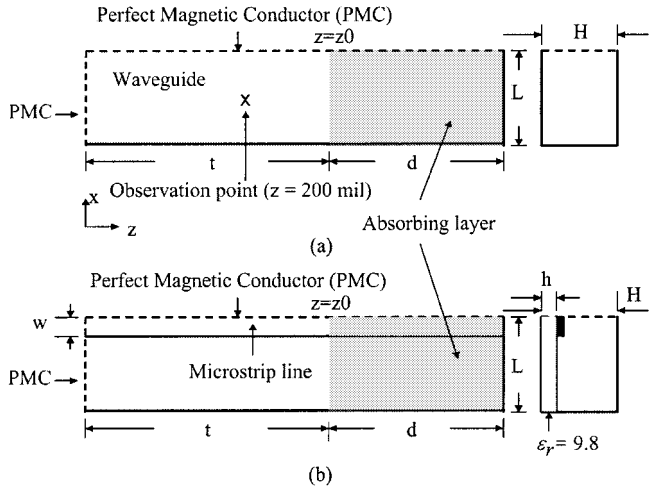

Fig. 1. Simulated half-regions of: (a) waveguide and (b) microstrip line using the perfectly matched anisotropic absorbing layer.

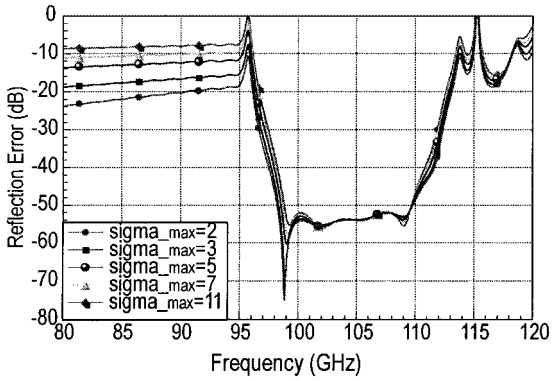

Fig. 2. Reflection error due to anisotropic PML termination of the waveguide structure in Fig. 1(a) for various values of $\sigma_{\max}(m = 2)$.

where $\underline{C}_d$ is the equivalent capacitance and $\underline{I}_d$ is the equivalent current source. Both of the above compose a Norton equivalent circuit of FETD cells as seen by the device. As the lumped-circuit model is used to represent the device, Kirchoff's law is applied to construct state equations, which are generally a system of first-order nonlinear ODEs, characterizing the EM wave and device interaction. The nonlinear ODE system is discretized with a forward difference scheme, and then the resulting equations are solved using multifrontal sparse Gaussian elimination, provided by the Harwell Subroutine Library, AEA Technology, Oxfordshire, U.K. For each time step, the updating of the electric field requires solving a matrix equation of the type $[A]X = [B]$, where $[A]$ is a sparse matrix. Since this matrix is not time dependent, it can be factorized once before time marching. The computation procedure of the mixed EM and circuit simulation algorithm can be summarized as follows. Assume all the electric field quantities of FETD cells are known at time steps $n-1$ and n, and they are used to set up the known forcing vector $[\underline{F}]$ in (14). $\underline{I}_d$ and $\underline{e}_c$ across the lumped elements at time step $n+1$ are obtained by simultaneous solution of the ODE system, and then are fed back into (11) to compute the electric field at every edge in the FETD cells at time step $n+1$. This time-stepping scheme is repeated until the observation point after the drain of the device records the complete output response.

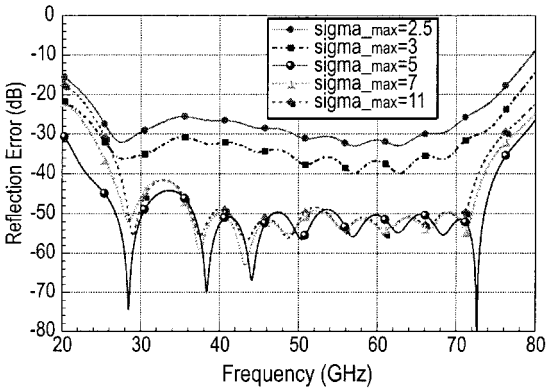

Fig. 3. Reflection error due to anisotropic PML termination of the microstrip line structure in Fig. 1(b) for various values of $\sigma_{\max}(m = 2)$.

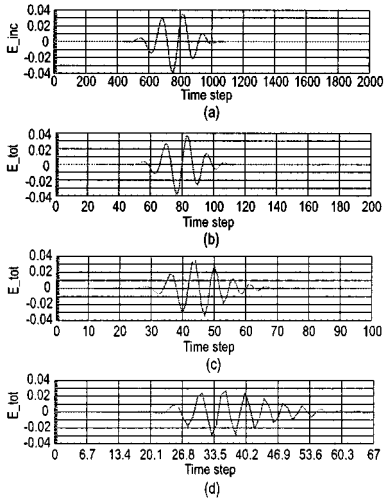

Fig. 4. Stability test in time-domain simulation for various values of time step. ($m = 2$, $\sigma_{\max} = 5$) The error increases as the step size is increased, but the solution is still stable. (a) Incident electric field $dt = dt_0$, $NT = 2000$. (b)–(d) Total electric field where: (b) $dt = 10\,dt_0$, $NT = 200$, (c) $dt = 20\,dt_0$, $NT = 100$, and (d) $dt = 30\,dt_0$, $NT = 67$. (dt_0 is the time-step size based on the stable criterion of the FDTD scheme. NT is the number of time step.)

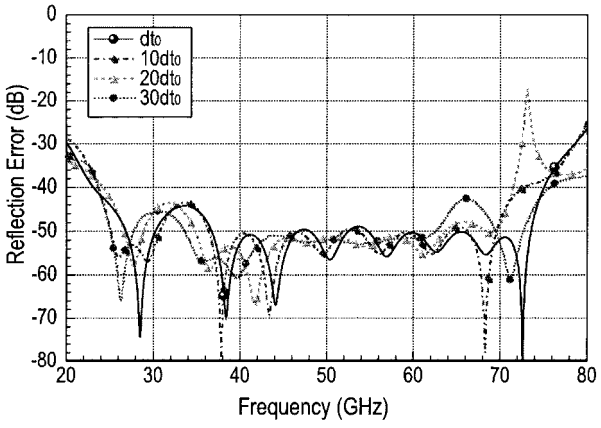

Fig. 5. Reflection error due to anisotropic PML termination of the microstrip line structure for various values of the time step ($m = 2$, $\sigma_{\max} = 5$.)

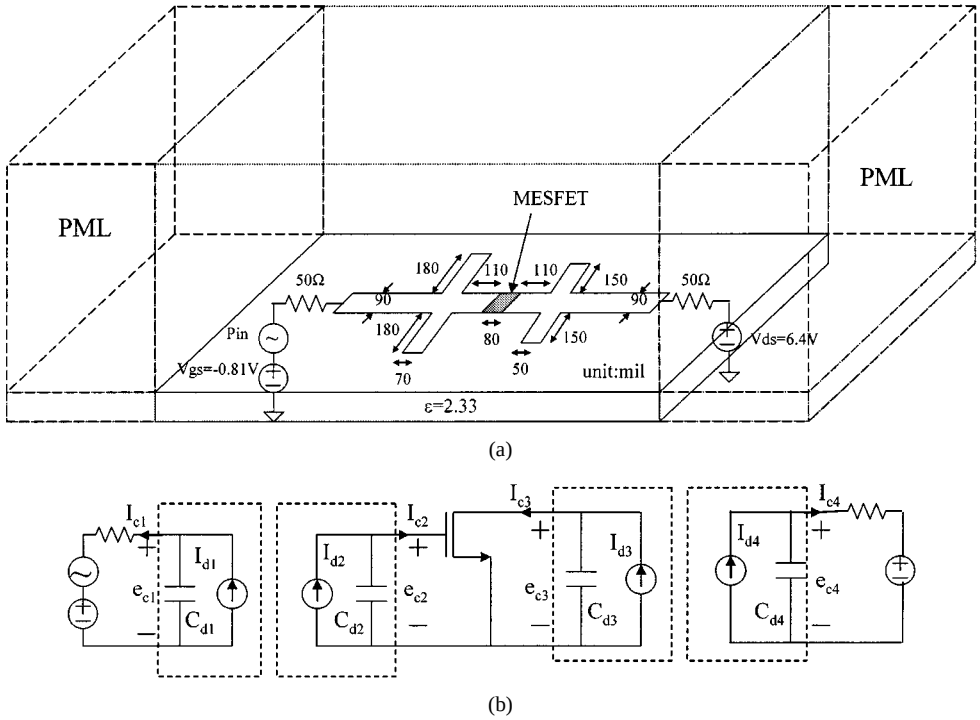

Fig. 6. (a) Simulation structure of the microwave amplifier. The circuit is metal shielded and the end wall is terminated by a ten-cell PML medium indicated by a long dashed box. (b) Equivalent circuit of the microwave amplifier. The passive structures are represented by Norton current sources and their internal capacitance are represented in dashed boxes, as seen from the active/passive device.

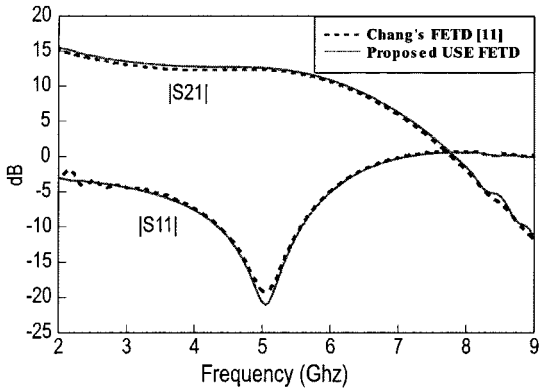

Fig. 7. Time response of the microwave amplifier.

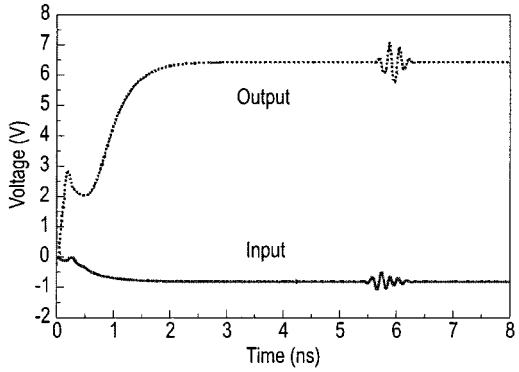

Fig. 8. Small-signal analysis of the microwave amplifier.

III. Result

A. PML Performance Test

To evaluate the performance of the proposed anisotropic PML, we consider the waveguide and shielded microstrip line shown in Fig. 1. The computation volume can be reduced to one-forth by setting perfect magnetic conductors (PMCs) at symmetric planes. The cross sections of the waveguide and the cavity shielding the microstrip line have the same dimensions, i.e., 50 mil $\times$ 74 mil. The microstrip line has 7.4-mil width, and the substrate has 7.4-mil thickness with a relative permittivity of 9.8. In both cases, the structures are terminated with a 200-mil-thick 20-layer absorber backing with PEC walls and the observation point is located at $z = 200$ mil, ten cells away from the interface of the PML. Our interest is to model the wave propagation in these structures and extract the reflection coefficient computed in the presence of the absorbing layer. Only the TE10 mode is chosen to propagate within the waveguide. The excitation of an electric probe consisting of a modulated Gaussian pulse is applied at the left-hand side, with $f0 = 104$ GHz and 10-GHz bandwidth for the waveguide and $f0 = 50$ GHz and 40-GHz bandwidth for the microstrip line. Berenger [16] found that if the conductivity is constant throughout the PML absorber, significant reflection occurs due to the discrete approximation of the field. The problem in the discrete space can be tempered by using a spatially variant along the normal axis as

$$\sigma(z) = \frac{\sigma_{\max}|z - z_0|^m}{\sqrt{\varepsilon_r}\, d^m} \tag{16}$$

where z_0 is the interface between the two medium, d is the depth of the PML, and m is the order of the polynomial variation.

For most of the cases that we have studied thus far, $m = 2$ is the appropriate order to minimize the reflection error. Figs. 2 and 3 show the reflection coefficients inside the waveguide and shielded microstrip line. A desired absorption down to -50 dB can be achieved by sufficient attenuation set by $\sigma_{\max}$, e.g., at least five for the microstrip line. A thinner absorber requires a higher $\sigma_{\max}$ to produce the same absorption.

Based on the stable criterion of the FDTD scheme, the time-step size of the microstrip line should be smaller than $dt_0 = 0.15$ ps, where $\Delta x_{\min} = 7.4$ mil, $\Delta y_{\min} = 1.85$ mil, and $\Delta z = 10$ mil. To prove the unconditional stability of the algorithm, we simulate the microstrip-line structure by increasing the time-step size up to 30 times dt_0. Fig. 4(a) shows the incident field in step size dt_0 for comparison. Fig. 4(b)–(d) shows the total field in various time-step sizes. The time-domain dispersion error increases as the step size is increased, but the solution is still stable. To reduce the dispersion error, higher order (third or fourth) time-domain descritization scheme can be used. Fig. 5 shows the reflection error due to anisotropic PML termination of the microstrip-line structure for various values of time step ($m = 2, \sigma_{\max} = 5$). When the step size is 30 times larger then dt_0, the solution still provides good accuracy. This algorithm remains stable as the step size is increased until the Nyquist rule is broken.

B. Analysis of Microwave Amplifier

Fig. 6(a) shows the layout of the simulated circuit using this technique. The system under consideration is a microwave amplifier, which includes a distributed passive structure, lumped passive device, and an active device (GaAs MESFET). Fig. 6(b) shows the equivalent circuit of the whole system. The distributed circuit can be simulated using an FETD algorithm and represented via the Norton generators with capacitive internal admittance. The value of the Norton sources and their internal capacitance is derived by the matrix equation (14). In this paper, we do not consider the propagation effect of EM fields inside the device because the device sizes are much smaller than the wavelength in most of cases. The passive and active devices can be represented by lumped-circuit models. Each circuit element is placed on the edge of an FETD cell as a two-terminal element. This mixed EM and circuit simulation algorithm has considered EM/circuit interaction at the following four locations:

1) input generators;
2) device input (gate) terminal;
3) output (drain) terminals;
4) load/drain power supply.

For comparison purposes, the active circuit (i.e., MESFET) used is the same as in Chang *et al.*'s FETD technique [13] and Kuo *et al.*'s extended FDTD technique in [9]. The large-signal model can be found in [9]. The dc-bias condition of this amplifier ($V_{\rm gs} = -0.81$ V and $V_{\rm ds} = 6.4$ V) is provided by the two power supplies connected at the input and output ports, respectively, while the RF source is represented by the generator connected to the input.

A FORTRAN program has been implemented. The entire simulation region is metal shielded and the end wall is terminated by a 400-mil-thick ten-layer absorber. σ is spacially variant as (15), while $m = 2$ and $\sigma_{\max} = 4$. A modulated Gaussian pulse with central frequency at 5 GHz is used to excite the circuit. The number of the unknown electric fields to be solved in this mesh is 303 198. The mesh has a minimum tetrahedral radius of $h = 25$ mil. When the time step size (3.5 ps) is ten times bigger than that in [13], the number of computation time steps is reduced to 2500. The simulation time are 7 h and 50 min on a PC Pentium II 450 MHz by using the standard FETD method in [13] and the proposed USE FETD method, respectively. Fig. 7 shows the time-domain response of the amplifier when a Gaussian modulated pulse is applied at its input. Fig. 8 shows a good comparison of the scattering parameters of the amplifier with the result obtained with the FETD method in [13] shown.

IV. CONCLUSION

In this paper, we have proposed a USE FETD method to solve a microwave passive/active circuit by adapting the lumped-element treatment. In addition, we have demonstrated an optimal anisotropic PML for the FETD to achieve a desired absorption down to -50 dB over a wide frequency band in two propagation problems. The USE FETD algorithm cooperated with the PML and was used here to analyze a microwave amplifier. The result not only retains the accuracy of the FETD method in [13], but also shows that the number of time iterations required can be significantly reduced. As the need for mixed EM and circuit simulation and computer-aided design (CAD) tools is going to increase in the future with development of a wide range of commercial products operating at a higher frequency, this implicit method is very competitive with an explicit method for the sake of geometry flexibility, accuracy, and efficiency.

ACKNOWLEDGMENT

Author Tsai wishes to thank S.-H. Chang, Broadcom Corporation, Irvine, CA, for his helpful discussion.

REFERENCES

[1] M. Righi, G. Tardioli, L. Cascio, and W. J. R. Hoefer, "Time-domain characterization of packaging effects via segmentation technique," *IEEE Trans. Microwave Theory Tech.*, vol. 45, pp. 1905–1910, Oct. 1997.

[2] K. M. Coperich, J. Morsey, V. I. Okhmatovski, A. C. Cangellaris, and A. E. Ruehli, "Systematic development of transmission-line models for interconnects with frequency-dependent losses," *IEEE Trans. Microwave Theory Tech.*, vol. 49, pp. 1677–1685, Oct. 2001.

[3] W. Sui, D. A. Christensen, and C. H. Durney, "Extending the two-dimensional FDTD method to hybrid electromagnetic systems with active and passive lumped elements," *IEEE Trans. Microwave Theory Tech.*, vol. 40, pp. 724–730, Apr. 1992.

[4] M. Piket-May, A. Taflove, and J. Baron, "FD-TD modeling of digital signal propagation in 3-D circuits with passive and active loads," *IEEE Trans. Microwave Theory Tech.*, vol. 42, pp. 1514–1523, Aug. 1994.

[5] V. A. Thomas, M. E. Jones, M. Piket-May, A. Taflove, and E. Harrigan, "The use of SPICE lumped circuits as sub-grid models for FDTD analysis," *IEEE Microwave Guided Wave Lett.*, vol. 4, pp. 141–143, May 1994.

[6] B. Toland, J. Lin, B. Houshmand, and I. Itoh, "Electromagnetic simulation of mode control of a two element active antenna," in *IEEE MTT-S Int. Microwave Symp. Dig.*, San Diego, CA, May 1994, pp. 883–886.

[7] C.-N. Kuo, V. A. Thomas, S. T. Chew, B. Houshmand, and T. Itoh, "Small-signal analysis of active circuits using FDTD algorithm," *IEEE Microwave Guided Wave Lett.*, vol. 5, pp. 216–218, July 1995.

[8] P. Ciampolini, P. Mezzanotte, L. Roselli, and R. Sorrentino, "Accurate and efficient circuit simulation with lumped-element FDTD technique," *IEEE Trans. Microwave Theory Tech.*, vol. 44, pp. 2207–2215, Dec. 1996.
[9] C.-N. Kuo, B. Houshmand, and T. Itoh, "Full-wave analysis of packaged microwave circuits with active and nonlinear devices: An FDTD approach," *IEEE Trans. Microwave Theory Tech.*, vol. 45, pp. 819–826, May 1997.
[10] M. Chen, W. R. Deal, B. Houshmand, and T. Itoh, "Global time-domain full-wave analysis of microwave FET oscillators and self-oscillating mixers," in *IEEE MTT-S Int. Microwave Symp. Dig.*, Baltimore, MD, June 1998, pp. 1135–1138.
[11] K. Guillouard, M. F. Wong, V. Fouad Hanna, and J. Citerne, "A new global finite-element analysis of microwave circuits including lumped elements," *IEEE Trans. Microwave Theory Tech.*, vol. 44, pp. 2587–2594, Dec. 1996.
[12] K. Guillouard, M. F. Wong, and V. Fouad Hanna, "A new global time domain electromagnetic simulator of microwave circuits including lumped elements based on finite element method," in *IEEE MTT-S Int. Microwave Symp. Dig.*, 1997, pp. 1239–1242.
[13] S.-H. Chang, R. Coccioli, Y. Qian, and T. Itoh, "A global finite-element time domain analysis of active nonlinear microwave," *IEEE Trans. Microwave Theory Tech.*, vol. 47, pp. 2410–2416, Dec. 1999.
[14] S. D. Gedney and U. Navsariwala, "A comparison of the performance of the FDTD, FETD, and planar generalized Yee algorithms on high performance parallel computers," *Int. J. Numer. Modeling*, vol. 8, pp. 265–276, May–Aug. 1995.
[15] A. D. Gedney and U. Navsariwala, "An unconditionally stable finite element time-domain solution of the vector wave equation," *IEEE Microwave Guided Wave Lett.*, vol. 5, pp. 332–334, Oct. 1995.
[16] J. P. Berenger, "A perfectly matched layer for the absorption of electromagnetic waves," *J. Comput. Phys.*, vol. 114, pp. 185–200, Oct. 1994.
[17] Z. S. Sacks, D. M. Kingsland, R. Lee, and J.-F. Lee, "A perfectly matched anisotropic absorber for use as an absorbing boundary condition," *IEEE Trans. Antennas Propagat.*, vol. 43, pp. 1460–1463, Dec. 1995.
[18] D. M. Kingsland, J. Gong, J. L. Volakis, and J.-F. Lee, "Performance of an anisotropic artificial for truncating finite-element method," *IEEE Trans. Antennas Propagat.*, vol. 44, pp. 975–981, July 1996.
[19] S. D. Gedney, "An anisotropic perfectly matched layer-absorbing medium for the truncation of FDTD lattices," *IEEE Trans. Antennas Propagat.*, vol. 44, pp. 1630–1639, Dec. 1996.
[20] V. Mathis, "An anisotropic perfectly matched layer-absorbing medium in finite element time domain method for Maxwell's equations," presented at the IEEE AP-S-URSI Presentation, Montreal, QC, Canada, 1997.
[21] A. Bossavit, "Whitney form: A class of finite elements for three-dimensional computations in electromagnetism," *Proc. Inst. Elect. Eng.*, pt. A, vol. 135, pp. 493–500, Nov. 1988.
[22] J. P. Webb, "Edge elements and what they can do for you," *IEEE Trans. Magn.*, vol. 29, pp. 1460–1465, Mar. 1993.
[23] N. M. Newmark, "A method of computation for structural dynamics," *J. Eng. Mechanics Division*, vol. 85, pp. 67–94, July 1959.
[24] O. C. Zienkiewicz, "A new look at the Newmark, Houboult and other time stepping formulas: A weighted residual approach," *Earthquake Eng. and Structural Dynamics*, vol. 5, pp. 413–418, 1977.

Hsiao-Ping Tsai (S'00) was born in Taiwan, R.O.C., in 1970. She received the B.S. and M.Sc. degrees in electrical engineering from the National Taiwan University, Taiwan, R.O.C., in 1994 and 1997, respectively, and is currently working toward the Ph.D. degree in electrical engineering at the University of California at Los Angeles (UCLA).

In 1998, she joined the Electrical Engineering Department, UCLA. Her research interests include time-domain global modeling of nonlinear semiconductor devices and microwave circuits.

Ms. Tsai was the recipient of the 2000 Honorable Mention Award in the Student Paper Competition of the IEEE Microwave Theory and Techniques Society (IEEE MTT-S) International Microwave Symposium.

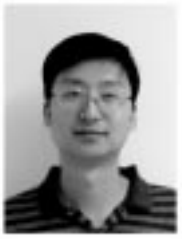

Yuanxun Wang (S'96–M'99) was born in Hubei, China, in 1973. He received the B.S. degree in electrical engineering from the University of Science and Technology of China (USTC), Hefei, China, in 1993, and the M.S. and Ph.D. degrees in electrical engineering from The University of Texas at Austin, in 1996 and 1999, respectively.

From 1995 to 1999, he was a Research Assistant with the Department of Electrical and Computer Engineering, The University of Texas at Austin. Since 1999, he has been with the Department of Electrical Engineering, University of California at Los Angeles (UCLA), where he is currently a Research Engineer and Lecturer. His research interests concern the enabling technology for RF and microwave front-ends in wireless communication and radar systems, as well as the numerical modeling, simulation, and feature-extraction techniques for microwave circuits, antennas, and EM scattering. He has authored or coauthored approximately 40 refereed journal and conference papers.

Tatsuo Itoh (S'69–M'69–SM'74–F'82) received the Ph.D. degree in electrical engineering from the University of Illinois at Urbana-Champaign, in 1969.

From September 1966 to April 1976, he was with the Electrical Engineering Department, University of Illinois at Urbana-Champaign. From April 1976 to August 1977, he was a Senior Research Engineer with the Radio Physics Laboratory, SRI International, Menlo Park, CA. From August 1977 to June 1978, he was an Associate Professor at the University of Kentucky, Lexington. In July 1978, he joined the faculty at The University of Texas at Austin, where he became a Professor of electrical engineering in 1981 and Director of the Electrical Engineering Research Laboratory in 1984. During the summer of 1979, he was a Guest Researcher at AEG-Telefunken, Ulm, Germany. In September 1983, he was selected to hold the Hayden Head Centennial Professorship of Engineering at The University of Texas at Austin. In September 1984, he was appointed Associate Chairman for Research and Planning of the Electrical and Computer Engineering Department, The University of Texas at Austin. In January 1991, he joined the University of California at Los Angeles (UCLA), as Professor of electrical engineering and Holder of the TRW Endowed Chair in Microwave and Millimeter Wave Electronics. He was an Honorary Visiting Professor at the Nanjing Institute of Technology, Nanjing, China, and at the Japan Defense Academy. In April 1994, he became an Adjunct Research Officer for the Communications Research Laboratory, Ministry of Post and Telecommunication, Japan. He currently holds a Visiting Professorship at The University of Leeds, Leeds, U.K., and is an External Examiner of the Graduate Program of the City University of Hong Kong. He has authored or coauthored 274 journal publications, 540 refereed conference presentations, and 30 books/book chapters in the area of microwaves, millimeter-waves, antennas and numerical electromagnetics. He has generated 49 Ph.D. students.

Dr. Itoh is a member of the Institute of Electronics and Communication Engineers of Japan and Commissions B and D of USNC/URSI. He became an Honorary Life Member of the IEEE Microwave Theory and Techniques Society (IEEE MTT-S) in 1994. He was the editor-in-chief of the IEEE TRANSACTIONS ON MICROWAVE THEORY AND TECHNIQUES (1983–1985) and the IEEE MICROWAVE AND GUIDED WAVE LETTERS (1991–1994). He serves on the Administrative Committee of the IEEE MTT-S. He was vice president of the IEEE MTT-S in 1989 and president in 1990. He was the chairman of USNC/URSI Commission D (1988–1990), and Chairman of Commission D of the International URSI (1993–1996). He is the chair of the Long Range Planning Committee of URSI. He serves on advisory boards and committees of a number of organizations. He has been the recipient of a number of awards, including the 1998 Shida Award presented by the Japanese Ministry of Post and Telecommunications, the 1998 Japan Microwave Prize, the 2000 IEEE Third Millennium Medal, and the 2000 IEEE MTT-S Distinguished Educator Award.